Prediction of discontinuous fatigue crack growth in high density polyethylene based on the crack layer theory with variable crack layer parameters

Jung-Wook Wee, Byoung-Ho Choi *

School of Mechanical Engineering, Korea University, Seoul 136-701, Republic of Korea

ABSTRACT

Crack layer (CL) theory has the advantage of capturing the physics of slow crack growth (SCG) and simulating various scenarios of SCG in thermoplastics. However, lack of knowledge regarding the dependency of CL input parameters on loading conditions and time limits the use of CL theory in predicting the lifespan of materials subject to brittle fracture. In this study, CL theory with variable average process zone (PZ) boundary traction (σ_{close}) and characteristic time for PZ degradation (t^*) is applied to fatigue tests with various loading conditions in order to observe discontinuous SCG. Using simulations, experimental results are achieved by changing two CL parameters, thereby establishing these two parameters as the key factors affecting SCG for various types of applied loads. In addition, the specific relationships between these two parameters and fatigue loading conditions are obtained. These obtained relationships may be beneficial for practical use of CL theory to estimate the SCG processes as well as their lifespan under various fatigue conditions.

© 2016 Elsevier Ltd. All rights reserved.

1. Introduction

Recently, high density polyethylene (HDPE) is widely used in water and natural gas distribution pipes. The expected lifespan of HDPE pipes is several decades in field conditions [1]. Owing to the long-term failure process of thermoplastic structural elements, accelerated experiments have been widely used in the laboratory setting [2,3]. Here, environmental and loading conditions may be manipulated to execute short-term testing through increasing temperature and load beyond their normally encountered values [4–7]. Specifically, cyclic loading is widely employed for accelerated testing of creep [8]. In these experiments, it is critical to identify the relationship between short-term experiments and long-term field failure processes, such as the connection between fatigue and creep failure. For this purpose, a comprehensive understanding of fracture mechanisms under various loading conditions is essential. The fracture mechanism of thermoplastics under fatigue including HDPE [1,9] varies as a function of applied stress, stress ratio, and frequency, as well as temperature and environment. The chain and molecular structures of HDPE undergo substantial breakage and recrystallization in the case of relatively high load conditions, which is known as ductile failure. Under lower load conditions, however, final failure may occur in the form

of brittle fracture without large amounts of plastic deformation, which is often observed in field failures of HDPE pipes. To obtain meaningful results, the variation in loading conditions of the accelerated testing must reflect the same fracture mechanisms of actual field failures.

Brittle fracture of HDPE can be conventionally divided into three stages during creep and fatigue loading conditions. In the first stage, micro-crazes accumulate in the vicinity of pre-existing defects. When the accumulated damage exceeds a specified critical level, a macroscopic crack starts to grow. In the second stage, the crack grows slowly in a brittle manner through a quasi-static crack growth process, also known as slow crack growth (SCG). Finally, in the third stage, global instability leads to catastrophic failure with rapid crack propagation (RCP) [10]. In many filed failure cases, the time for SCG is considered the major contribution of the lifespan of HDPE. Therefore, accurate modeling of the SCG process is critical to predicting the lifespan of HDPE. Hence, many studies have been conducted to investigate the SCG process of HDPE [2,3,10–13]. Evidently, SCG of HDPE proceeds in a continuous or discontinuous manner depending on the applied load, temperature, and crack size. Differences in SCG patterns are accompanied by significantly different SCG kinetics. The point at which the mechanism and kinetics of the SCG distinctly change is referred to as the ductile-brittle transition of the second kind (DBT2), since it corresponds to the transition from ductile (creep) to brittle fracture of the microfibers within the process zone (PZ) [2,9,12,14,15].

* Corresponding author.
E-mail address: bhchoi@korea.ac.kr (B.-H. Choi).

There are several empirical models of SCG rate based on the conventional Paris law [16–18]. However, these modified models still do not competently capture the discontinuous SCG mode of HDPE. This can be plainly seen from the fact that the empirical models use the crack driving force exclusively, i.e., the stress intensity factor, without consideration for the interaction between the crack and PZ [10]. Morphological and microstructural studies on the crack as well as the PZ in front of the crack tip are necessary to address these shortcomings. The crack layer (CL) theory is the first model that allows the PZ to evolve independently of the crack and explicitly considers the interaction between the main crack and PZ (namely, damages ahead of crack tip). The system including the main crack and PZ, which surrounds the crack tip, comprises the CL [19]. In the case of engineering thermoplastics, localized strain areas (damage) surrounding the main crack tip may vary, depending on the molecular architecture and morphology of the polymer in addition to the stress state [20]. Polyethylene (PE), especially HDPE, displays a simple wedge shape PZ, consisting of cold drawn fibers and membranes, with a relatively sharp boundary between the PZ and the surrounding original material. Therefore, in this case a superposition method is applicable. It enables simplification of the CL parameters [13,21,22]. That is, the morphological characteristics of the PZ and crack can be utilized to construct CL theory for simulating SCG behavior of various thermoplastics, including HDPE.

During the CL simulation, several parameters reflecting the material properties, microstructure, and test conditions were employed, e.g., the closing stress acting on PZ boundary, the initial surface fracture energy, the enthalpy transition for material transformation, and the natural drawing ratio, amongst others. Although each CL parameter has a clear physical meaning, the experimental evaluation of such parameters are commonly required. So, the application of CL theory for prediction of thermoplastic lifespan in brittle fracture is somewhat limited. One effective way of improving the applicability of CL theory is to conduct a systematic analysis of the correlations between SCG behavior and various CL parameters. An investigation on the effect of temperature, which is one of the accelerating factors, on the enthalpy of cold drawing, i.e. material transformation from its original isotropic state to a highly oriented drawn status, was performed [9]. However, studies on the other CL parameters are also necessary.

In this study, a parametric analysis was performed to estimate the lifespan and SCG mode of field conditions through a combination of short-term tests and numerical simulations of SCG and PE lifespan. SCG behavior of HDPE under fatigue loading conditions was numerically simulated by applying CL theory. A variation of CL input parameters was considered for the parametric analysis. The experimental results reported by Parsons et al. [2,12] were compared with our simulation results, and the CL parameter dependency on fatigue loading conditions, such as maximum load level, R-ratio, and loading frequency, were constructed. Since that the CL theory suggests a system of two coupled differential equations describing the crack and PZ evolution, the phenomenological observations used in the present study can be extended to other conditions, as long as the crack-PZ interaction mechanism is the same. Therefore, one can accurately estimate the SCG behavior and the lifespan of HDPE at fatigue and creep loading conditions through application of the CL algorithm presented in this study.

2. Theoretical background and simulations

2.1. Application of crack layer theory to HDPE

The CL is a system including the main crack and surrounding damage zone, which is often called the PZ [23]. The typical mor-

phology of wedge-shaped PZ in HDPE is shown in Fig. 1 [13]. The increase in damage density as a function of time is explained as a decrease in surface fracture energy (SFE), serving as the resistance to crack propagation. The propagation of a main crack through a PZ is determined by the competition between the driving force for crack propagation and the corresponding resistance.

The crack tip and the process zone tip can be defined clearly in case of HDPE due to its typical shape of PZ as shown in Fig. 2. PZ can form in front of the crack tip once the remote load applied, and it means that highly drawn PZ can be considered as a transformed material from undamaged HDPE. The potential energy variation due to such transformation can be represented as the variation of Gibbs potential energy (G) between original and PZ materials [11,23]. The variation of Gibbs potential energy (G) with PZ movement can be also calculated under the condition that the PZ and remaining material are considered to be distinct phases. Under this assumption, the driving force for PZ growth (X^{PZ}) can be expressed as shown in Eq. (1). Applying this to the crack propagation, the corresponding driving force (X^{CR}) can be obtained as shown in Eq. (2). Here, the crack and PZ growth rate can be calculated by employing the appropriate linear relationships [21].

$$X^{PZ} = -\frac{\delta G}{\delta l_{PZ}}\bigg|_{l_{CR}=const.} = J_1^{PZ} - \gamma^{tr}R_1, \tag{1}$$

$$X^{CR} = -\frac{\delta G}{\delta l_{CR}}\bigg|_{l_{PZ}=const.} = J_1^{CR} - 2\gamma, \tag{2}$$

where l_{PZ} and l_{CR} are the length of the PZ and the crack, and J_1^{PZ} and J_1^{CR} are the energy release rate (ERR) for the PZ and the crack growth, respectively. γ^{tr} is the enthalpy density difference between the transformed material and original one. R_1 is the volumetric quantity of material transformed from the original material to the PZ. It is indicative of a dissimilarity with the Dugdale-Barenblatt (DB) model, based on the condition that $K_{tot} = 0$ to accomplish an equilibrium, which means that $X^{PZ} = 0$ [24,25]. Since this model does not consider the enthalpy requirements for the material transformation into PZ material per unit volume, γ^{tr}, there have been several results indicating the inaccuracy of the DB model for cases of polymeric materials accompanying large energy dissipation [13,26]. γ is the SFE of transformed material, degrading with time. It is worth noting that each equation is nonlinear, and the equations for PZ and crack growth are combining each other, having multiple degrees of freedom. Thus, a numerical solving process, simplified according to the observed PZ features, is necessary for the pragmatic use of the CL simulation.

As shown in Fig. 1, HDPE shows a simple narrow wedge shape of the PZ, and materials in the PZ can be considered as second-phase homogeneous, i.e. highly drawn polymer. These characteristics facilitate the further simplification of CL model through introducing the method of superposition [11,13,21]. In Fig. 2, the PZ cutoff material can be thought as an elastic material, and the quantity of transformed material is calculated using the natural drawing ratio (λ) and crack opening displacement (δ_{tot}) at the crack tip. The simplified driving force for PZ growth is as follows [13].

$$X^{PZ} = J_1^{PZ} - \gamma^{tr}R_1 = \frac{K_{tot}^2}{E'} - \frac{\gamma^{tr}}{\lambda - 1}\delta_{tot}|_{x=l}, \tag{3}$$

where K_{tot} and δ_{tot} stand for the stress intensity factor (SIF) at the PZ tip and crack opening displacement (COD) at the crack tip, respectively, and are determined by employing the superposition of the external load and the boundary stress distributed from the crack tip to the PZ tip (Fig. 2). In addition, E' is the elastic modulus in plane strain condition.
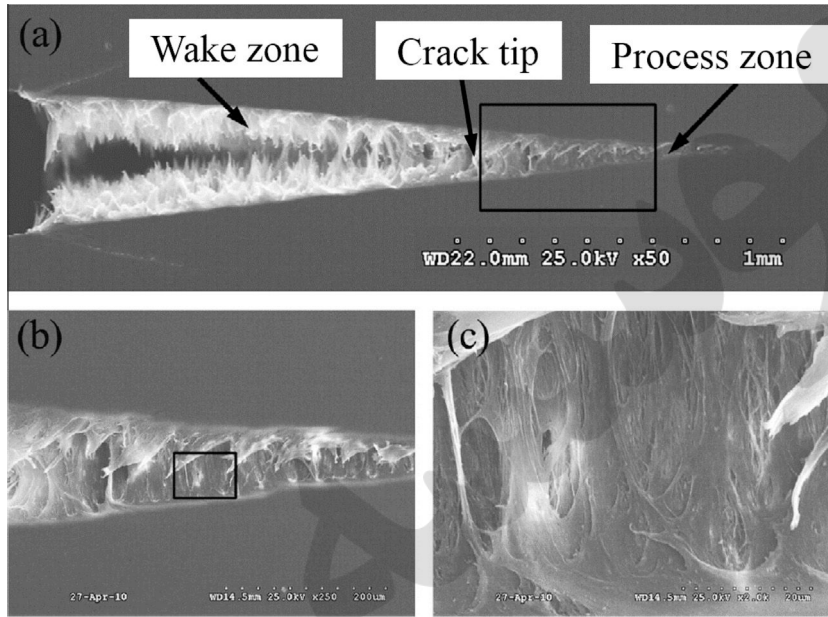
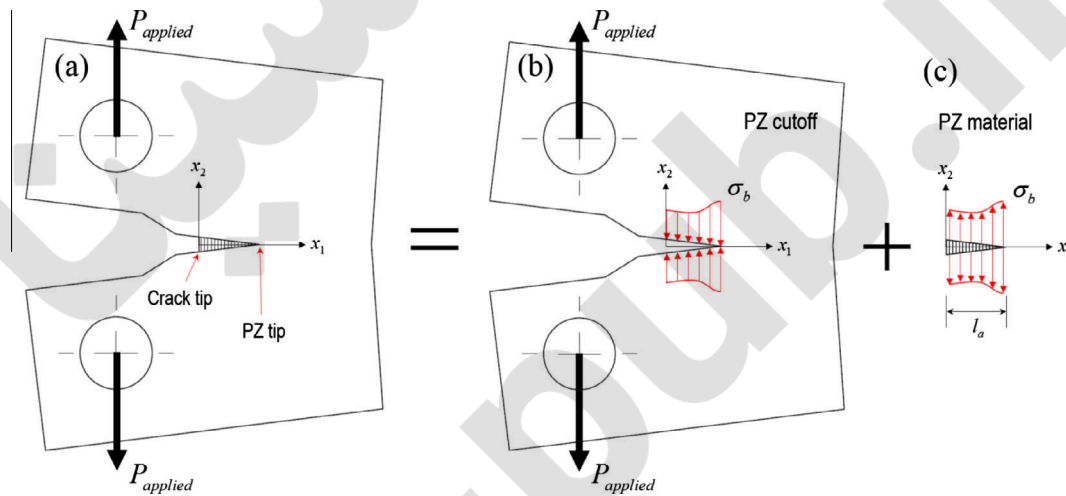**Fig. 1.** Typical process zone (PZ) feature of HDPE [13].

Fig. 2. Schematics of the method of superposition in CT specimen (The boundary stress σ_b will be a function of position, x_1 and other factors such as loading conditions, and temperature).

The exact distribution of the boundary stress has yet to be clarified. The actual boundary traction may be related to the yield stress (σ_Y) and drawing stress (σ_{dr}) of HDPE, suggesting a rate dependency of the PZ boundary traction. To facilitate modeling, the distribution of the boundary traction can be treated as a uniform closing stress of the average value of the boundary stress, σ_{close}, which is larger than the drawing stress [11]. The closing stress can be calculated as the average value of boundary stress acting around the PZ (i.e. average of σ_b of shown in Fig. 2). Indeed, the closing stress is not a material property, and varies with specimen geometry, loading conditions, and temperature, amongst other factors. Therefore, elucidating the effect of these conditions on σ_{close} is critical.

Further simplification of CL simulations using HDPE can be accomplished by addressing surface fracture energy (SFE). As seen in Fig. 1, the transformed material in the PZ shows highly fibrillated features, and can be considered an anisotropic homogeneous material with mechanical degradation. Therefore, a model for SFE degradation can be applied to the entire homogeneous AZ material as Eq. (4) below [3].

$$\gamma = \gamma_0 \frac{1}{1 + \left(\frac{t_i}{t^*}\right)^r}, \tag{4}$$

where γ_0 is the initial SFE of the original material and t_i is the elapsed time from the beginning of the material degradation. t^* is the characteristic time for degradation, and r is a positive fitting factor. As seen from Eq. (4), the SFE decreases as a function of degradation time and t^* controls the speed of SFE reduction. The smaller the value of t^*, the faster the SFE degrades. The speed of SFE degradation also depends on the loading conditions. That is, the value of t^* can be changed with fatigue loading conditions, as well as σ_{close}. Understanding the effect of fatigue and creep loading conditions on the closing stress and characteristic time, and identifying the relationships between them are the primary goals of this research.

2.2. Simulation of SCG based on CL theory

Based on the description of CL theory for HDPE, a numerical simulation is programmed using the commercial software MATLAB, and the algorithm of the program is shown in Fig. 3. To verify the contribution of fatigue loading conditions including the R-ratio, scale of applied load, and loading frequency to t^* and σ_{close}, the discontinuous SCG simulations were compared with experimental results, adopted from the studies of Parsons et al. [2,12]. Thirteen experimental results were used with varied $K_{I,max}$

and R-ratio values with a 1 Hz load frequency, and four results were used for frequency variation with constant $K_{I,max}$ and R-ratio values. Sinusoidal cyclic loads were applied for fatigue tests. These experiments revealed the fracture surfaces with discontinuous striations and the time to the first and second step jump times (t_1, t_2), and final failure time (t_f). The applied load scale in the fatigue condition was based on the maximum applied load, to achieve the applicability of the same model even using a fully reversed load ($R = -1$). A compact tension (CT) specimen with the same dimensions as the experiment specimens was used in
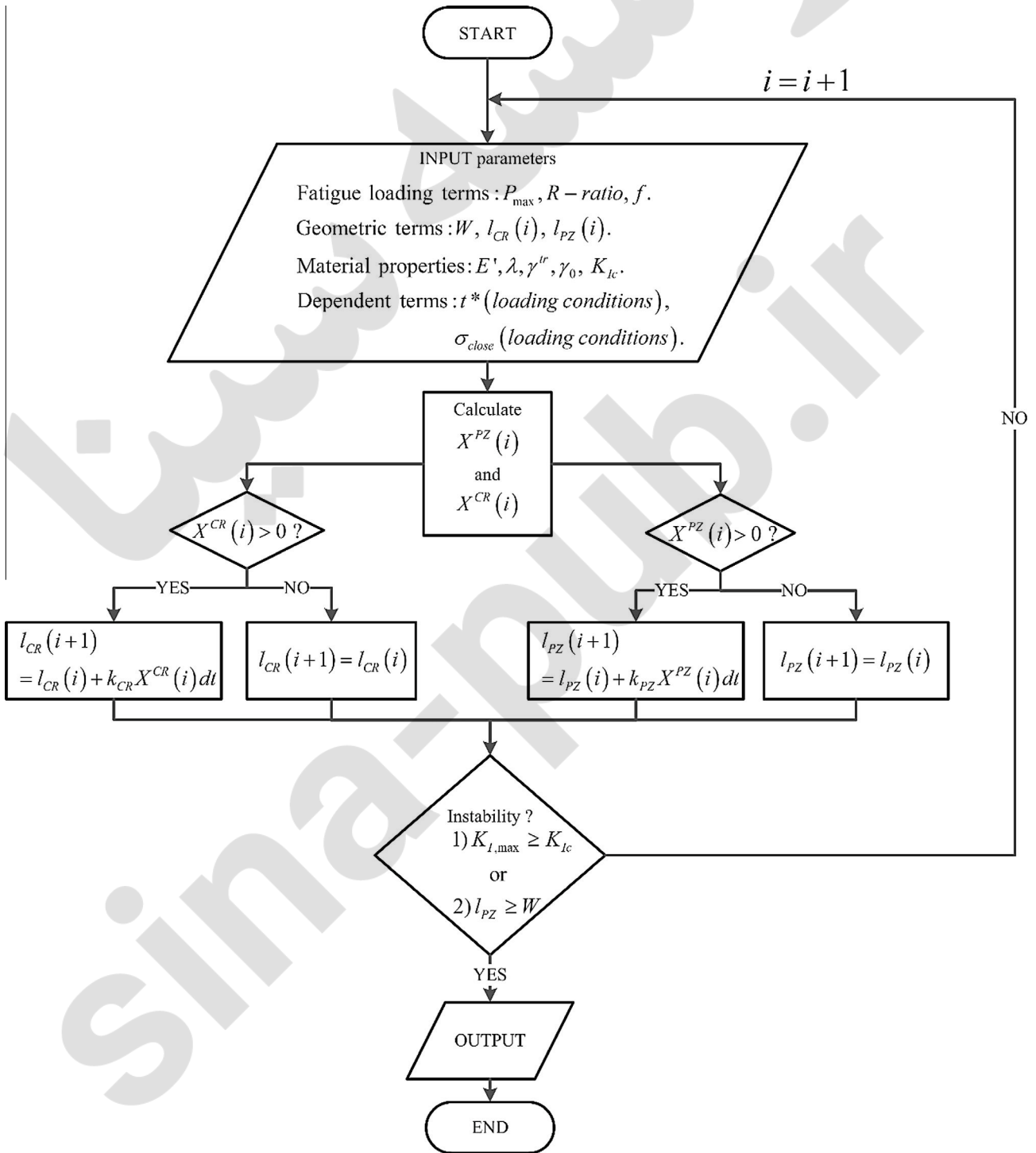

Fig. 3. Algorithm of the numerical simulation of SCG of HDPE based on the CL theory.

the CL simulation. From the experiments demonstrating the step-wise crack growth, the test results for the step jump length (Δl_i), and the times to the step jump (t_1, t_2, t_f) were matched by the CL simulation as shown in Fig. 4 with only t^* and σ_{close} differing. The two failure criteria of the CL simulation were employed in the present study. The first was the point at which the K_I at the crack tip exceeds the fracture toughness, $K_{I,C}$ of HDPE. In this case, fast fracture occurs. The second was the point at which all remaining ligaments transform into PZ material. Under this condition, the PZ material acts like a plastic hinge and the CT specimen is characterized by a high degree of rotation.

3. Results and discussion

3.1. Comparison of simulation results and test results

The experimental results of various fatigue loading conditions, including fracture surface, were reproduced with changes only in
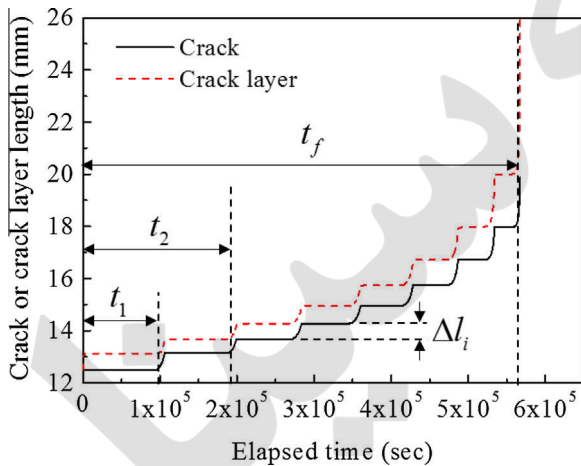

Fig. 4. Definition of the incubation time ($t_1, t_2 \ldots$) and the varied crack length for typical discontinuous SCG behaviors of HDPE.

the t^* and σ_{close} values. Fig. 5 shows the test results [2] and simulations with various $K_{I,max}$ and R-ratio values, at a constant loading frequency of 1 Hz. All step lengths were well-fitted with their experimental counterparts. The time required for step jumps of the CL simulation was also similar to that of the experiments, which is listed in Table 1.

Fig. 6 displays the comparison between the fracture surfaces of the experiments and those of the CL simulation at four different loading frequencies (0.01, 0.1, 0.2, 1 Hz). Fig. 7 gives the time to the step jump obtained from test and simulation results. The R-ratio and $K_{I,max}$ remained constant as 0.1 and 1.30 MPa $\sqrt{m}$, respectively. Discontinuous step lengths and times to the step jump of the simulations were in a good agreement with the test results as well.

The entire discontinuous SCG process and corresponding surface fracture energy (2γ) degradation are respectively shown in Figs. 8 and 9 for the cases of 1, 0.1, 0.01 Hz loading frequencies. A main crack began to develop when the energy release rate at the crack tip (J_1^{CR}) was larger than 2γ, indicating the positive crack driving force (X^{CR}). After the crack propagated through the sufficiently degraded PZ material, the crack tip encountered the intact material having an initial surface fracture energy ($2\gamma_0$), and was again arrested until the new material degraded enough to achieve a positive X^{CR} value. The sudden jumps in Fig. 9 were matched with the crack jumps, while gradual degradations corresponded to the crack arrest times. Therefore, as the crack propagation path increased, the J_1^{CR} at each crack end point also increased; hence, the required degradation time reduced as a function of crack propagation. This demonstrates the discontinuous SCG concept. As is well known, a rise in frequency leads to a rise in fatigue life in terms of the number of cycles [27]. When the time of failure is reached, on the contrary, the frequency increase generates a decrease in lifespan [28]. Those characteristics are well illustrated in Fig. 8(a) and (b) with fully discontinuous SCG behavior, indicating the validity of the CL methodology.

This demonstrates that the CL simulation is applicable to all discontinuous SCG processes, as well as the lifespan prediction of various fatigue and creep conditions with various load scales, R-ratios,
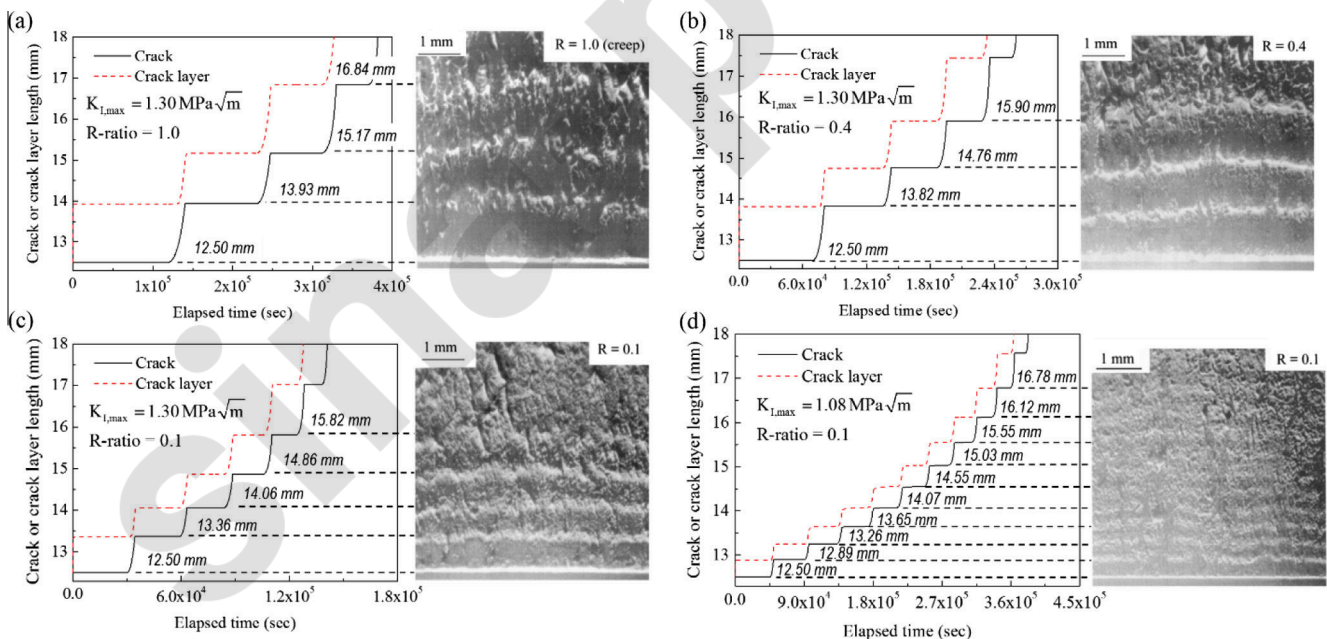

Fig. 5. Discontinuous slow crack growth (SCG) obtained from crack layer (CL) simulation and corresponding fracture surface with various $K_{I,max}$ and R-ratio, indicating well suited simulation with experiments. (Micrographs of fracture surface striations are adopted from Parsons et al. [2] with permission).

Table 1
Experimental and simulation results of time to first, second step jumps and failure time with variation of $K_{I,max}$ and R-ratio at a constant frequency, 1 Hz. Experimental results are adopted from Ref. [2].

R-ratio	$K_{I,max}$ (MPa $\sqrt{m}$)	Experimental t_1 (10^3 s)	CL simulation t_1 (10^3 s)	Experimental t_2 (10^3 s)	CL simulation t_2 (10^3 s)	Experimental t_f (10^3 s)	CL simulation t_f (10^3 s)
0.1	1.30	32 ± 2	30.2	58 ± 2	59.59	153 ± 19	146.7
0.4	1.30	70 ± 7	69.9	138 ± 11	135.3	264 ± 35	261.9
0.8	1.30	94 ± 2	98.8	176 ± 2	188.2	383 ± 34	340.6
1.0	1.30	135 ± 21	120.2	220 ± 14	231.7	403 ± 52	382.7
0.1	1.08	48 ± 4	45.8	85 ± 7	91.4	386 ± 34	396.8
0.32	1.08	98 ± 15	95.6	169 ± 15	188.2	590 ± 32	567.7
0.5	1.08	123 ± 16	127.2	213 ± 38	249.2	660 ± 55	659.0
1.0	1.08	168 ± 11	191.1	278 ± 4	370.0	864 ± 61	698.2
0.2	1.43	33 ± 3	30.2	60 ± 7	58.5	135 ± 2	134.9
0.3	1.30	54 ± 16	52.1	103 ± 18	102.5	228 ± 32	230.2
0.5	1.13	121 ± 8	106.1	196 ± 8	208.2	570 ± 3	581.0
1.0	0.85	421 ± 30	382.6	701 ± 2	741.9	2065 ± 290	1860
0.22	1.17	64 ± 4	57.7	114 ± 8	114.0	297 ± 25	338.8

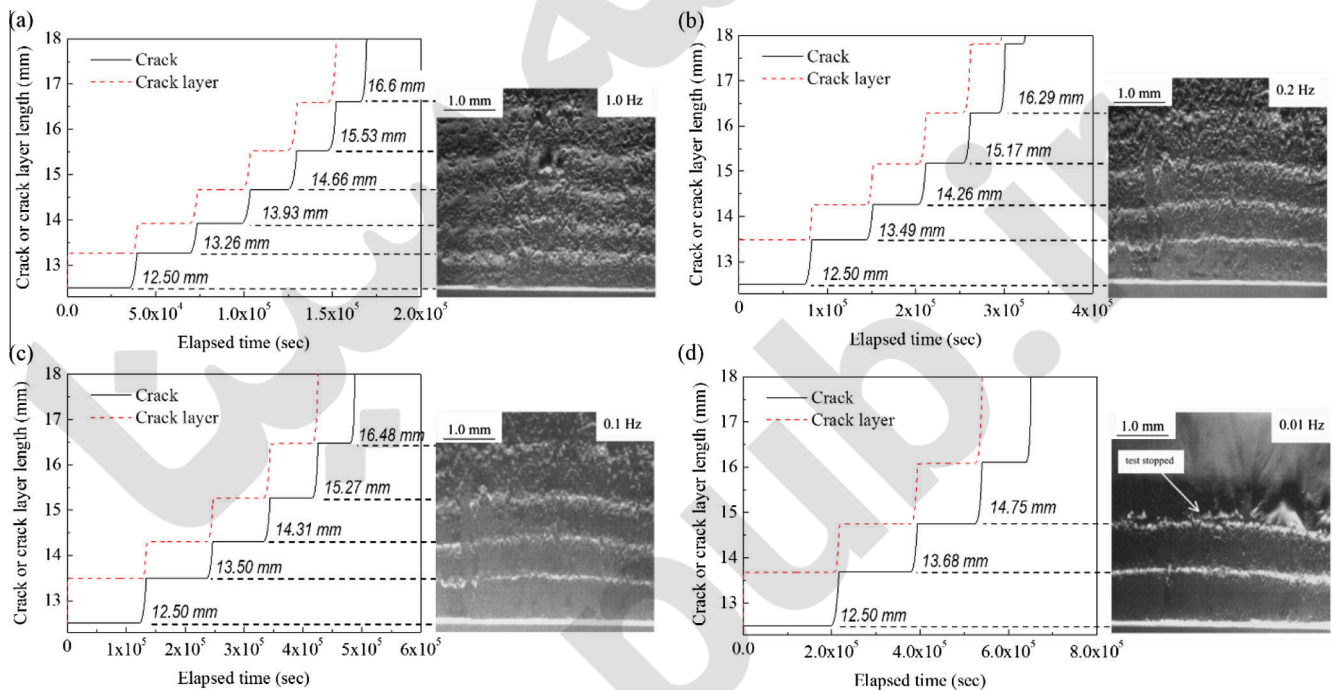Loading frequency, f = 1 Hz.

Fig. 6. Discontinuous slow crack growth (SCG) obtained from crack layer (CL) simulation and corresponding fracture surface at a various frequencies ((a) 0.01, (b) 0.1, (c) 0.2 and (d) 1 Hz), indicating well suited simulation with experiments. R-ratio and $K_{I,max}$ are 0.1 and 1.30 MPa m$^{0.5}$ respectively. (Micrographs of fracture surface striations are adopted from Parsons et al. [12] with permission).
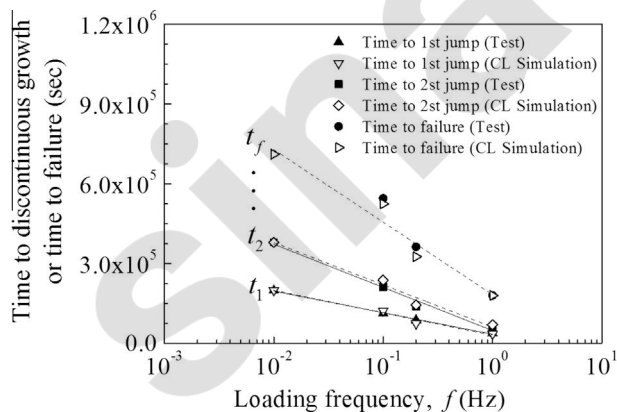

Fig. 7. Experimental and simulation results of time to first, second step jumps and time to failure with variation of loading frequency at constant $K_{I,max}$ (1.30 MPa m$^{0.5}$) and R-ratio = 0.1. (Experimental results are adopted from Parsons et al. [12]).

and loading frequencies. The creep tests (R = 1.0) were effectively simulated also using the same CL simulation methodologies. In addition, the favorably reproduced results revealed that the two parameters, t^* and σ_{close}, are critical to accurately simulating the SCG procedures and lifespan in cyclic and creep loading conditions.

3.2. Variation of parameters with fatigue loading conditions

3.2.1. Characteristic time (t^*)

As mentioned, t^* controls the degradation speed of the PZ material. Since aggressive environments are not considered in the current study, the degradation mechanisms primarily occur by mechanical degradation from fatigue or creep. Because the applied frequencies are substantially less than or equal to 1 Hz, hysteretic localized heating was not considered. Regarding fatigue conditions, it is well known that the high loads and low R-ratios, indicating large stress fluctuation, decreases the fatigue lifespan [2]. In
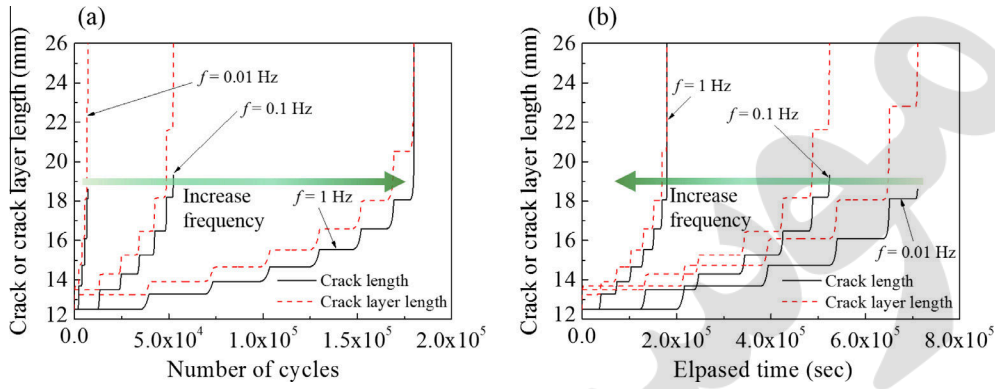
Fig. 8. Crack and crack layer propagation with various fatigue frequencies (f = 1, 0.1, 0.01 Hz). (a) Crack and crack layer length with number of cycles and (b) crack and crack layer length with time.
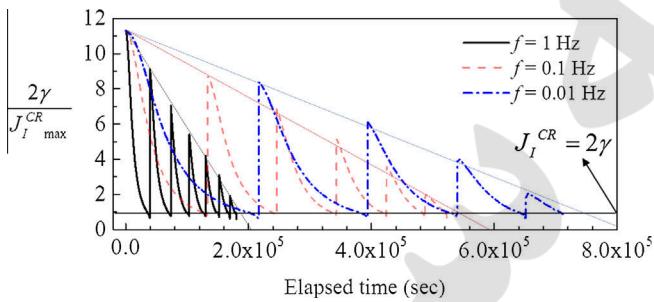

Fig. 9. Variation of surface fracture energy normalized with energy release rate at crack tip, at different frequencies.
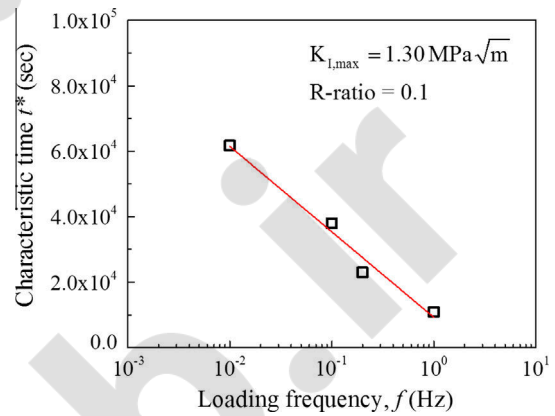

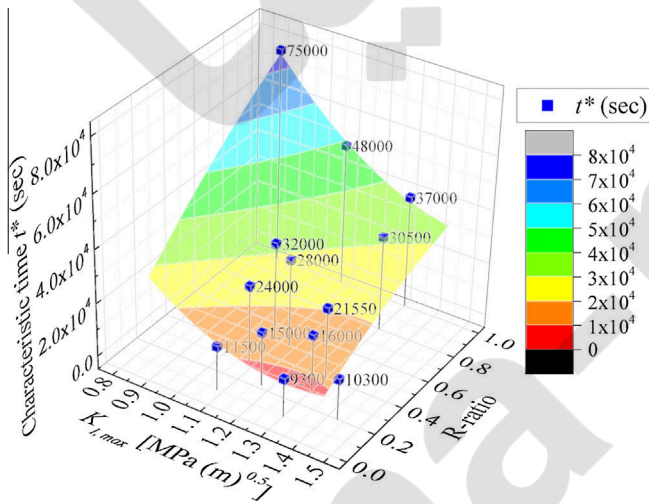**Fig. 11.** Characteristic time t^* with loading frequency f. (The unit of f is Hz).

Fig. 10. Variation of characteristic time t^* with $K_{I,\max}$ and R-ratio at the frequency of 1 Hz.

addition, a higher frequency causes a lifespan reduction in terms of time, not the number of cycles [12]. The factors affecting the degradation rate, correspondingly, are $K_{I,\max}$, R-ratio, and frequency of applied load consequently.

Fig. 10 shows the variation of t^* with R-ratio and $K_{I,\max}$ at a loading frequency of 1 Hz. This surface plot illustrates the above statements. At a given R-ratio, an increase in $K_{I,\max}$ results in a reduction of t^*, indicating faster SFE degradation. Similarly, a decrease in the R-ratio at a given $K_{I,\max}$, which is associated with an increase in the amount of load fluctuation, results in a decrease of t^* based on the

same concept. During creep, the case in which the R-ratio has a value of one, t^* also decreases with increasing applied load.

The surface fitting equation is as follows. The variation of t^* with $K_{I,\max}$ and R-ratio is well-fitted using a quadratic 2D equation.

$$t^*(K_{1,\max}, R) = 158,900 - 242,400K_{1,\max} + 105,900R$$
$$+ 94,220K_{1,\max}^2 - 13,960R^2 - 45,580K_{1,\max}R \qquad (5)$$

Fig. 11 illustrates the change of t^* with variation of loading frequency. When fatigue load is applied with high frequency, the drop in SFE by mechanical degradation is accelerated and is represented as a decrease in t^*. From Fig. 11, it can be seen that there is an inverse proportionality between t^* and log scale frequency as follows.

$$t^* \sim \log\left(\frac{1}{f}\right) \qquad (6)$$

Eqs. (5) and (6) may be used as a practical tool to estimate the value of t^* in any reasonable fatigue range of structural HDPE elements.

3.2.2. Closing stress (σ_{close})

Similar to t^*, the averaging boundary traction σ_{close} varied with the test conditions, such as specimen type, temperature, and fatigue loading, amongst others. The drawing process of the AZ material was characteristic of cold drawing phenomena observed in tensile tests [29,30]. Therefore, the behavior of σ_{close} in response to external loads can be considered analogously with tensile behavior of thermoplastics. This means that the σ_{close} can be thought of as a adjustable parameter based on applied loading
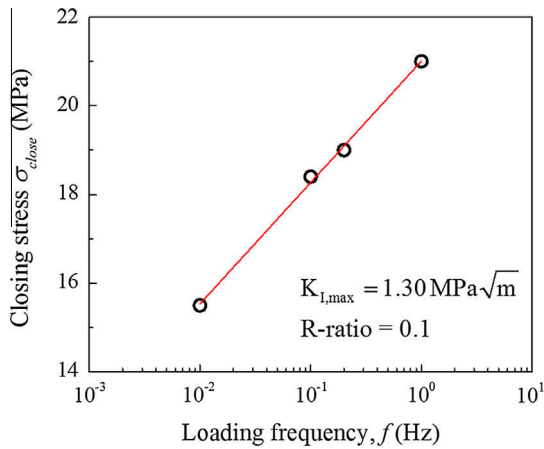
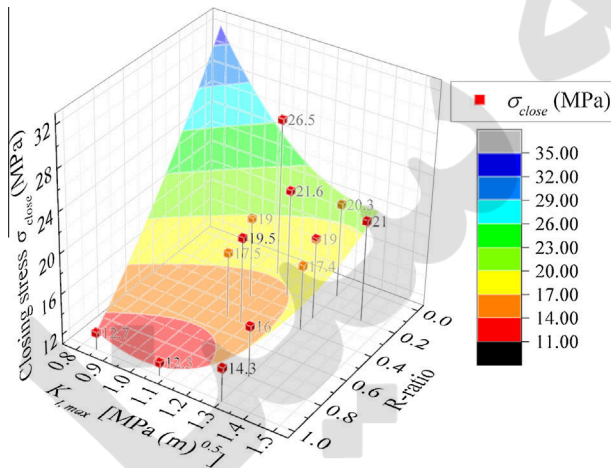**Fig. 12.** Closing stress with loading frequency f. (The unit of f is Hz).

Fig. 13. Variation of closing stress with $K_{I,\mathrm{max}}$ and R-ratio at a frequency of 1 Hz.

stress, and reduction of ductility. Furthermore, modeling the strain rate at crazes in the vicinity of the crack tip has shown it to be related to fatigue frequency [12]. Therefore, in can be reasonably assumed that σ_{close} increases with increasing frequency of the applied load. This behavior is well represented in Fig. 12. As expected, σ_{close} increases with increasing frequency f. The obtained relationship between σ_{close} and frequency f is as follows.

$$\sigma_{\mathrm{close}} \sim \log(f) \tag{7}$$

There is also a linear relationship between σ_{close} and logarithmic f, proving that the frequency f contributes to both σ_{close} and t^* logarithmically.

Fig. 13 illustrates the 3D plot of σ_{close} as a function of $K_{1,\mathrm{max}}$ and R-ratio at a frequency of 1 Hz. There is no consistent relationship between σ_{close} and $K_{1,\mathrm{max}}$, at a constant R-ratio. This dependency differs through varying R-ratio values. σ_{close}, seems rather closely related with R-ratio. These tendencies are clearly shown in Fig. 14 and in the partial 2d plots of Fig. 13. At a given R-ratio, the variation of closing stress demonstrates an inconsistent trend with $K_{1,\mathrm{max}}$. However, at a given $K_{1,\mathrm{max}}$, the closing stress demonstrates a consistent trend with R-ratio. This signifies that the closing stress, the average boundary stress of fibrils in the PZ, is indeed related to the normalized fluctuation of the load, which can be expressed using the R-ratio term. The described frequency and R-ratio dependency for strain rate of fibrils stands in agreement with a previously suggested model [12]. The 3D fitting equation $\sigma_{\mathrm{close}}(K_{1,\mathrm{max}}, R - \mathrm{ratio})$ was also obtainable as follows.

$$\sigma_{\mathrm{close}}(K_{I,\mathrm{max}}, R) = 106.6 - 116.9K_{I,\mathrm{max}} - 59.43R + 40.28K_{I,\mathrm{max}}^2$$
$$+ 6.232R^2 + 34.93K_{I,\mathrm{max}}R \tag{8}$$

From the above four relationships, $t^*(K_{1,\mathrm{max}}, R), t^*(f)$, $\sigma_{\mathrm{close}}(K_{1,\mathrm{max}}, R)$, and $\sigma_{\mathrm{close}}(f)$, long-term lifespan prediction, as well as SCG behavior of HDPE material in field conditions can be identified.

4. Conclusion

Since CL theory has various input parameters, it is difficult to use. In this study, fatigue and creep conditions of SCG in HDPE were well simulated using CL theory, and demonstrated good agreement with experiments. The step length and time to step jumps were well-fitted by controlling the average PZ boundary traction (σ_{close}) and characteristic time (t^*) for material degradation. From the two parameter approach, four useful correlations were obtained, i.e. $t^*(K_{1,\mathrm{max}}, R), t^*(f), \sigma_{\mathrm{close}}(K_{1,\mathrm{max}}, R), \sigma_{\mathrm{close}}(f)$, which correspond well with the proposed physical concepts.

conditions, particularly strain rate. It is well known that HDPE material shows strain rate dependency similar to common polymers [31,32].

Due to the viscoelastic nature of HDPE, the overall boundary traction distribution may increase with increasing strain rate. It is accepted that increased frequency of the fatigue test results in the same effect as increased strain rate on the test material [27,33]. This also indicates the increase in yield stress, drawing
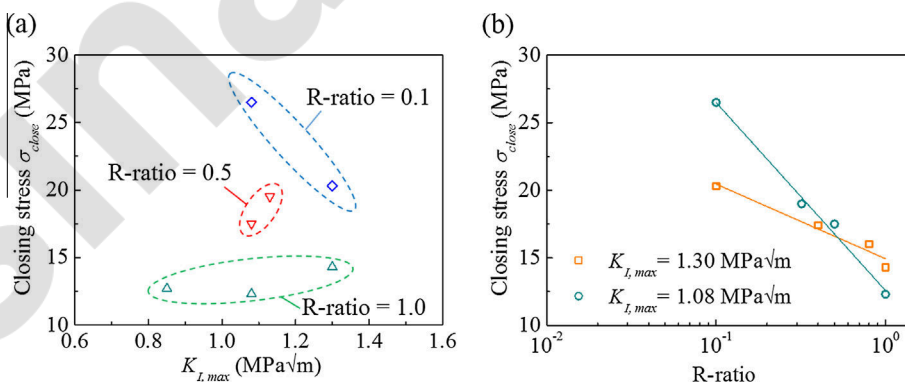

Fig. 14. Partial plots of 3d surface plot shown in Fig. 13. (a) At a given R-ratio, the consistent tendency of closing stress with $K_{1,\mathrm{max}}$ is unnoticeable. On the contrary, (b) there are consistent R-ratio dependency of closing stress at a given $K_{1,\mathrm{max}}$.

This article demonstrates three desirable points for the practical utilization of CL theory for SCG behaviors of HDPE. First, it confirms the wide applicability of CL theory to diverse loading conditions by showing the accurate simulation of SCG of HDPE with proper failure mechanism changes, i.e. continuous and discontinuous SCG behaviors. Second, for various fatigue loading conditions, the experimental data can be reproduced very precisely by simply varying two CL parameters, i.e. characteristic time and closing stress. That is, those two CL parameters can be key factors for effectively simulating HDPE under fatigue and creep conditions. Finally, the SCG pattern and lifespan of various fatigue and creep loadings can be predicted using CL theory, through utilization of the four proposed equations. These findings may be advantageous to engineers designing with thermoplastics.

Acknowledgement

References

[1] Chudnovsky A, Shulkin Y, Baron D, Lin K. New method of lifetime prediction for brittle fracture of polyethylene. J Appl Polym Sci 1995;56:1465–78.
[2] Parsons M, Stepanov E, Hiltner A, Baer E. Correlation of stepwise fatigue and creep slow crack growth in high density polyethylene. J Mater Sci 1999;34:3315–26.
[3] Choi B-H, Balika W, Chudnovsky A, Pinter G, Lang RW. The use of crack layer theory to predict the lifetime of the fatigue crack growth of high density polyethylene. Polym Eng Sci 2009;49:1421.
[4] Han M-H, Narin JA. Hygrothermal aging of polyimide matrix composites laminates. Compos Part A – Appl S 2003;34:979–86.
[5] Lubineau G, Violeau D, Ladeveze P. Illustrations of a microdamage model for laminates under oxidizing thermal cycling. Compos Sci Technol 2009;69:3–9.
[6] Choi B-H, Chudnovsky A, Paradkar R, Michie W, Zhou Z, Cham P-M. Experimental and theoretical investigation of stress corrosion crack (SCC) growth of polyethylene pipes. Polym Degrad Stab 2009;94:859–67.
[7] Quino G, Yagoubi JE, Lubinineau G. Characterizing the toughness of an epoxy resin after wet aging using compact tension specimens with non-uniform moisture content. Polym Degrad Stab 2014;109:319–26.
[8] Kasakevich M, Moet A, Chudnovsky A. Comparative crack layer analysis of fatigue and creep crack propagation in high density polyethylene. Polymer 1990;31:435–9.
[9] Chudnovsky A, Zhou Z, Zhang H, Sehanobish K. Lifetime assessment of engineering thermoplastics. Int J Eng Sci 2012;59:108–39.
[10] Chudnovsky A. Slow crack growth, its modeling and crack-layer approach: a review. Int J Eng Sci 2014;83:6–41.
[11] Chudnovsky A, Shulkin Y. Application of the crack layer theory to modeling of slow crack growth in polyethylene. Int J Fract 1999;97:83–102.
[12] Parsons M, Stepanov E, Hiltner A, Baer E. Effect of strain rate on stepwise fatigue and creep slow crack growth in high density polyethylene. J Mater Sci 2000;35:1857–66.
[13] Zhang H, Zhou Z, Chudnovsky A. Applying the crack-layer concept to modeling of slow crack growth in polyethylene. Int J Eng Sci 2014;83:42–56.
[14] Lu X, Qian R, Brown N. Discontinuous crack growth in polyethylene under a constant load. J Mater Sci 1991;26:917–24.
[15] Lu X, Brown N. A test for slow crack growth failure in polyethylene under a constant load. Polym Test 1992;11:309–19.
[16] Paris P, Erdogan F. A critical analysis of crack propagation laws. J Basic Eng 1963;85:528–33.
[17] Forman RG, Kearney V, Engle R. Numerical analysis of crack propagation in cyclic-loaded structures. J Basic Eng 1967;89:459–63.
[18] Erdogan F, Ratwani M. Fatigue and fracture of cylindrical shells containing a circumferential crack. Int J Fract 1970;6:379–92.
[19] Chudnovsky A, Moet A. Thermodynamics of translational crack layer propagation. J Mater Sci 1985;20:630–5.
[20] Botsis J, Chudnovsky A, Moet A. Fatigue crack layer propagation in polystyrene—part I experimental observations. Int J Fract 1987;33:263–76.
[21] Kadota K, Chudnovsky A. Constitutive equations of crack layer growth. Polym Eng Sci 1992;32:1097–104.
[22] Stojimirovic A, Chudnovsky A. A new thermodynamic model for a process zone in polymers. Int J Fract 1992;57:281–9.
[23] Chudnovsky A. Crack layer theory. NASA contractor report 174634. Lewis Research Center; 1984.
[24] Dugdale D. Yielding of steel sheets containing slits. J Mech Phys Solids 1960;8:100–4.
[25] Barenblatt GI. The formation of equilibrium cracks during brittle fracture. General ideas and hypotheses. Axially-symmetric cracks. J Appl Math Mech 1959;23:622–36.
[26] Stojimirovic A, Kadota K, Chudnovsky A. An equilibrial process zone in polymeric materials. J Appl Polym Sci 1992;46:1051–6.
[27] Arad S, Radon J, Culver L. Strain rate dependence of failure processes in polycarbonate and nylon. J Appl Polym Sci 1973;17:1467–78.
[28] Arad S, Radon J, Culvcr L. Fatigue crack propagation in polymethylmethacrylate; the effect of loading frequency. J Mech Eng Sci 1972;14:328–34.
[29] Schirrer R, Masson JL, Tomatis B, Lang R. The disentanglement time of the craze fibrils under cyclic loading. Polym Eng Sci 1984;24:820–4.
[30] Rose L, Channell A, Frye C, Capaccio G. Slow crack growth in polyethylene: a novel predictive model based on the creep of craze fibrils. J Appl Polym Sci 1994;54:2119–24.
[31] Zhang C, Moore ID. Nonlinear mechanical response of high density polyethylene. Part I: Experimental investigation and model evaluation. Polym Eng Sci 1997;37:404–13.
[32] Dusunceli N, Colak OU. The effects of manufacturing techniques on viscoelastic and viscoplastic behavior of high density polyethylene (HDPE). Mater Des 2008;29:1117–24.
[33] Hertzberg R, Manson J, Skibo M. Frequency sensitivity of fatigue processes in polymeric solids. Polym Eng Sci 1975;15:252–60.